

## Colorimetric biosensing of glucose in human serum based on the intrinsic oxidase activity of hollow MnO<sub>2</sub> nanoparticles

Lijuan Chen <sup>a,b,c</sup>, Haiyan Gao <sup>a,b,c</sup>, Yan Bai <sup>a,b,c</sup>, Wei Wei <sup>a,b,c</sup>, Junfeng Wang <sup>d</sup>, Georges El Fakhri <sup>d,\*</sup>, and Meiyun Wang <sup>a,b,c,\*</sup>

<sup>a</sup>Department of Medical Imaging, Henan Provincial People's Hospital & People's Hospital of Zhengzhou University, Zhengzhou, Henan, 450003, China.

<sup>b</sup>Henan Key Laboratory for Medical Imaging of Neurological Diseases, Henan Provincial People's Hospital & People's Hospital of Zhengzhou University, Zhengzhou, Henan, 450003, China

<sup>c</sup>School of Clinical Medicine, Henan University, Zhengzhou, Henan, 450003, China.

<sup>d</sup>Gordon Center for Medical Imaging, Radiology, Massachusetts General Hospital, Harvard Medical School, 125 Nashua Street, Boston, MA, 02114

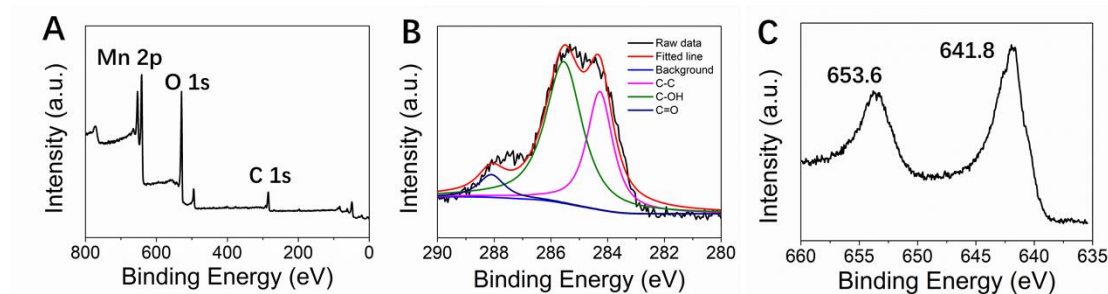


**Fig. S1.** (A) XPS full-scan spectra, (B) high-resolution C 1s and (C) high-resolution Mn 2p XPS spectra of H-MnO<sub>2</sub> NPs.

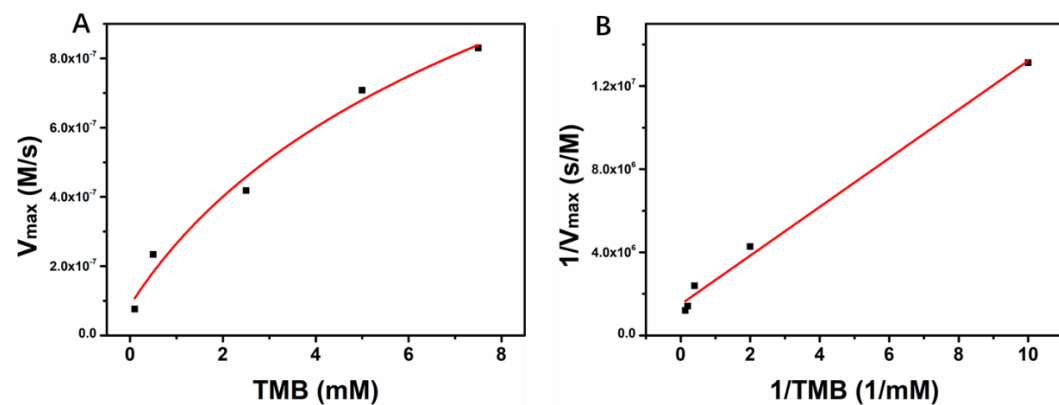


**Fig. S2.** The initial velocities in the oxidization of TMB were measured at pH 4.0. (A) Kinetic plot of  $v$  against TMB concentration. (B) Double-reciprocal plot generated from (A).

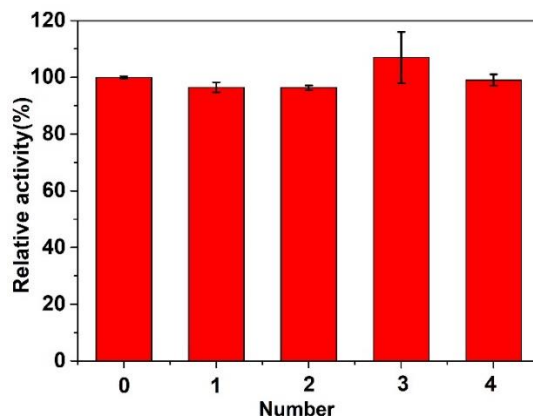


**Fig. S3.** The relative activity of H-MnO<sub>2</sub>. (Number 0 stands for the activity of H-MnO<sub>2</sub> NPs before nearly a year. The Number 1-4 stand for the current activity of H-MnO<sub>2</sub> NPs)

**Table S1.** Comparison of the kinetic parameters between H-MnO<sub>2</sub> NPs and other materials.  $V_{max}$  is the maximum rate of conversion,  $K_m$  is the Michaelis constant.

Catalyst	$K_m$ /mM	$V_{max}/\mu\text{M s}^{-1}$	Reference
H-MnO <sub>2</sub>	0.781	0.668	This work
Fe <sub>3</sub> O <sub>4</sub>	0.098	0.0344	[1]
CeO <sub>2</sub>	3.8	0.7	[1]
MnO <sub>2</sub> -Silk films	1.62	2.66	[2]
PANi-MnO <sub>2</sub> -Pd NWs	0.13	0.30	[3]
ZnFe <sub>2</sub> O <sub>4</sub> MNPs	0.85	0.13	[4]
CuZnFeS NCs	2.2	0.39	[5]

**Table S2.** Comparison of the performance of our method with other biosensors for measuring glucose concentration in human serum samples.

Biosensor	Linear range ( $\mu\text{M}$ )	LOD ( $\mu\text{M}$ )	Reference
GOx@ZIF-8(NiPd)	10-300	9.2	[6]
VS <sub>2</sub> nanosheets	5-250	1.5	[7]
Au NPs	2-200	0.5	[8]
GOx-Cu nanoflower	10-200	3.5	[9]
Carbon dots	200-2500	60	[10]
H-MnO <sub>2</sub> NPs	1-200	0.84	This work

## References

1. Liu X., Wang Q., Zhao H., Zhang L. Su Y., Lv Y., *Analyst*, 2012,137, 4552-4558.
2. Singh M, Bharadwaj K, Dey ES, Dicko C. *Ultrason Sonochem.* 2020, 64,105011.
3. Zhong M., Chi M., Ma F., Zhu Y., Wang C., Lu X., *ACS Sustainable Chem. Eng.* 2018, 6, 12,

- 16482-16492.
4. Ghosh, A. B.; Saha, N.; Sarkar, A.; Dutta, A. K.; Biswas, P.; Nag, K.; Adhikary, B. *New J. Chem.* 2016, 40, 1595-1604.
  5. Wei, H.; Wang, E. *Anal. Chem.* 2008, 80, 2250-2254.
  6. Q. Wang, X. Zhang, L. Huang, Z. Zhang, S. Dong, *Angew. Chem. Int. Ed.*, 2017,56(50):16082-16085.
  7. L. Huang, W. Zhu, W. Zhang, K. Chen, J. Wang, R. Wang, Q. Yang, N. Hu, Y. Suo, J. Wang, *Microchimica Acta*, 2018, 185(1): 1-8.
  8. Y. Jv, B. Li, R. Cao, *Chem. Commun.*, 2010, 46(42): 8017-8019.
  9. B.S. Batule, K.S. Park, S. Gautam, H.J. Cheon, M.I. Kim, H.G. Park, *Sens. Actuators B-Chem.*, 2019, 283,749-754.
  10. B. Wang, F. Liu, Y. Wu, Y. Chen, B. Weng, C.M. Li, *Sens. Actuators B-Chem.*, 2018,255, 2601-2607.